Compensation of Geometric Distortions in Multispectral Imaging: Effects on Sharpness and Color Accuracy

Julie Klein
Institute of Imaging and Computer Vision
RWTH Aachen University, 52056 Aachen, Germany
tel: +49 241 80 27860, fax: +49 241 80 22200
web: www.lfb.rwth-aachen.de

in: Proceedings of the 15th International Student Conference on Electrical Engineering POSTER 2011.
See also BibTeX entry below.

BibTeX:

```
@inproceedings{KLE11b,
  author = {Julie Klein},
  title = {Compensation of Geometric Distortions in Multispectral Imaging:
   Effects on Sharpness and Color Accuracy},
  booktitle = {Proceedings of the 15th International Student Conference on Electrical Engineering POSTER 2011},
  address = {Prague, Czech Republic},
  month = {May 12},
  year = {2011},
}
```

Compensation of Geometric Distortions in Multispectral Imaging: Effects on Sharpness and Color Accuracy

Julie KLEIN

Institute of Imaging and Computer Vision, RWTH Aachen University, 52056 Aachen, Germany

Julie.Klein@LFB.rwth-aachen.de

Abstract. *In multispectral imaging systems featuring a monochrome camera and bandpass color filters placed in front of it, geometrical distortions can not be avoided. Since the thicknesses, refraction indices and tilt angles of the optical filters are different, the images obtained with each of these filters exhibit some aberrations. The aberrations have already been modeled and can be measured and compensated. However, the compensation of the distortions also requires some interpolation step using the neighboring gray values of each pixel position. This inevitably leads to damages on the multispectral image: it can not be as sharp as the original image and this introduced blur also affects the color accuracy of the acquired multispectral image. In this paper, we will compare three different interpolation methods and analyze their consequences on the blur and on the color accuracy of the compensated images. We will show that sharpness and accurate color acquisition can not be optimized with the same interpolation method.*

Keywords

Multispectral imaging, transversal aberrations compensation, interpolation, spectral channels sharpness, spectral accuracy, image quality.

1. Introduction

Multispectral imaging allows a spectrally accurate acquisition of a scene: the spectral stimuli are not sampled by three broadband color channels like in an RGB camera, but the whole wavelength range is more finely sampled using, e. g., five to thirteen optical bandpass filters [1, 2, 3]. Moreover, using such spectral channels enables the Luther's law [4] to be verified. It states that an elementary transformation has to exist between the spectral sensitivity curves of the camera color channels and those of the cones present in the human retina in order to ensure an accurate acquisition of colors. Once the spectral sensitivity of the multispectral camera has been measured [5], the emission spectra of the scenes of interest can be estimated from the acquired color channels - i. e., from the different monochrome images acquired through the bandpass color filters in the case of a multispectral camera featuring filters - using a Wiener estimation for instance.

One particular way to sample the visible wavelength range and acquire several different color channels is the utilization of bandpass filters positioned between the monochrome sensor and the lens [6]. The color filters contained in our multispectral camera shown in Fig. 1 are included in a motorized filter wheel and have central wavelengths going from 400 to 700 nm in steps of 50 nm and their bandwidths are about 40 nm. Due to the different refraction indices, thicknesses and tilt angles of those filters – a perfect alignment of the filters in the filter wheel is practically impossible –, the optical paths of the rays coming from the acquired scene and reaching the sensor are altered and differ from one color channel to another. This results in two sorts of aberrations. The *transversal* aberrations concern the lateral displacement of the rays in the sensor plane: the image points corresponding to one object point in the different color channels are shifted, resulting in color fringes, principally on the edges in the image. The properties of the color filters cause also a displacement of the focus plane: the acquired scene can not be in focus in all the color channels with the same lens settings. These *longitudinal* aberrations are analyzed in [7] and cause blurring in the multispectral image.

Fig. 1. Multispectral camera utilized at our institute. Seven optical bandpass filters in a filter wheel are placed between a monochrome sensor and a lens.

To compensate for the transversal aberrations, a physical model has been developed [6]. Once the distortions have been measured, some interpolations must be performed on the gray values of the different color channels of the multispectral image, in order to undistort them. Up to now, a straightforward bilinear interpolation has been utilized. The blurring effects of interpolation methods are well known and can lead to some artifacts, as described by Tsao [8] and Rohde et al. [9]. In this work, we will examine the effects of the bilinear interpolation from the compensation on the blur of the undistorted multispectral image and on its color accuracy, and compare them with those obtained using other interpolations like the bicubic interpolation and the spline interpolation.

The structure of this paper is the following. First, the calculation of the transversal aberrations and their compensation are explained, with the different methods for the interpolation utilized in this paper for the compensation in Sec. 2.3. The consequences of the different interpolation methods on the sharpness and on the color quality of the multispectral images are showed in Sec. 3 and 4 respectively, and conclusions are drawn in Sec. 5.

2. Transversal Aberrations and their Compensation

In the following section, an overview over the physical modeling of the transversal aberrations and their compensation as they are performed at our institute is given. The transversal aberrations are considered separately from the longitudinal aberrations here, since the consequences of their compensation on the quality of the image concerning the sharpness and the color will be exposed.

2.1. Physical Model of Transversal Aberrations and their Calculation

The transversal aberrations induced by the optical filters in the ray path that exhibit different refraction indices, thicknesses or tilt angles and the physical modeling of these aberrations have been thoroughly exposed by Brauers et al. [6]. This subsection will roughly summarize these results. Figure 2 explains how transversal aberrations appear when a color filter is placed between the lens and the sensor plane. Due to the refraction index of the optical filter, the rays are refracted twice and the image point on the sensor is therefore shifted compared to the image point obtained when no optical filter is used.

Since our multispectral camera contains a filter wheel with the seven color filters (see Fig. 1), we have no access to the case in which no filter is in the ray path. We thus pick one color channel as a reference color channel (generally the color channel in the middle of the wavelength range, which is the one with the central wavelength 550 nm) and define the transversal aberration relative to this reference color channel.

The other color channels are compared to the reference channel using image registration. The similarity cri-

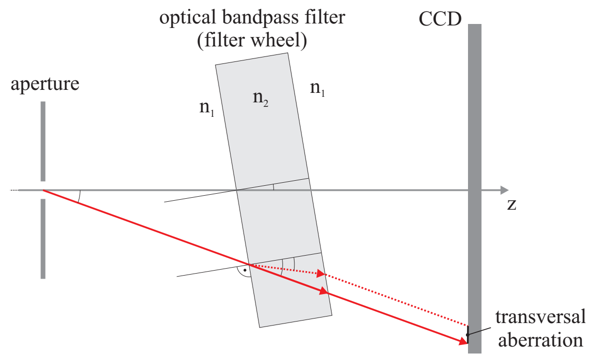

Fig. 2. The transversal aberrations are due to the insertion of a color filter in the ray path. The rays coming from the scene on the left are refracted and reach the sensor plane at a given position (dotted red rays). Without any filter, the rays would have reached the sensor at a different position (solid red rays). These aberrations also occur when two filters with different thicknesses, tilt angles or refraction indices are utilized.

terion utilized is the mutual information: the different color channels can exhibit some contrast inversion and the camera transfer function is possibly not linear and the mutual information gives good results in this case [6]. The color channels images are registered by taking either the whole images or smaller parts of the images. The mutual information is maximized using an iterative search algorithm and the application of different geometric transformations according to the physical model developed. The parameters of the model are then calculated using these registrations results.

2.2. Aberrations Compensation

Once the transversal aberrations have been measured, their compensation is performed as follows. Since the compensated image should be equidistantly sampled, the compensation starts from the pixel coordinates (x_c, y_c) in the sought corrected image and calculates the corresponding pixel coordinates (x_s, y_s) in the original distorted image using

$$\begin{pmatrix} x_s \\ y_s \end{pmatrix} = \mathbf{T} \cdot \begin{pmatrix} x_c \\ y_c \\ 1 \end{pmatrix} \tag{1}$$

with a different geometric transformation matrix $\mathbf{T} \in \mathbb{R}^{2\times 3}$ for each color channel. An example of transformation matrix for the color channel corresponding to the central wavelength 400 nm is

$$\mathbf{T} = \begin{pmatrix} 0.9978 & 0.0024 & 5.1983 \\ 0.0007 & 0.9968 & 0.7562 \end{pmatrix}. \tag{2}$$

Of course, for the reference color channel (central wavelength 550 nm), the transformation $\mathbf{T}$ is an identity matrix of size 2×3.

The gray value in the original distorted image at the position (x_s, y_s) is then transferred to the pixel position

(x_c, y_c) in the corrected image. The position (x_s, y_s) is not an entire pixel position and the corresponding gray value must thus be approximated by some interpolation using the neighboring gray values. This very step of the compensation and its consequences on the image quality are analyzed in this paper.

2.3. Interpolation Methods used for the Compensation

Currently, we use the straightforward bilinear interpolation during the compensation of transversal aberrations in multispectral image, but other methods could be used. Three interpolations are tested in this paper: the bilinear, the bicubic and the spline interpolation. They were performed with the `interp2` function of Matlab.

For the bilinear interpolation, the distorted image i_s is approximated around the position (x_s, y_s) using the following linear function

$$i_s(x, y) = \sum_{i=0}^{1} \sum_{j=0}^{1} l_{i,j} \cdot x^i \cdot y^j \tag{3}$$

where $l_{i,j}$ are four coefficients that are calculated using the known gray values of the four pixels around the position (x_s, y_s).

In a similar way, the bicubic interpolation utilizes the approximation

$$i_s(x, y) = \sum_{i=0}^{3} \sum_{j=0}^{3} c_{i,j} \cdot x^i \cdot y^j \tag{4}$$

around the position (x_s, y_s). The sixteen coefficients $c_{i,j}$ are calculated using assumptions about the first derivative of the approximating function and about its slopes at the pixel positions.

The spline interpolation utilized here is a cubic spline interpolation. A cubic spline is a piecewise polynomial whose pieces are connected in such a way that it and its first and second derivatives are continuous [10].

3. Effects of Interpolation on Blurring

To analyze how the sharpness of multispectral images is affected by the different interpolation methods used in the compensation step, we utilized an *artificial* multispectral image of a Gaussian noise. This means that we generated a multispectral image with a noise image of 500×500 pixels that we replicated seven times to get seven color channels. We weighted the color channels with different coefficients to get a reference gray image of Gaussian noise of $500 \times 500 \times 7$ pixels. A part of this multispectral image can be seen in Fig. 3(a).

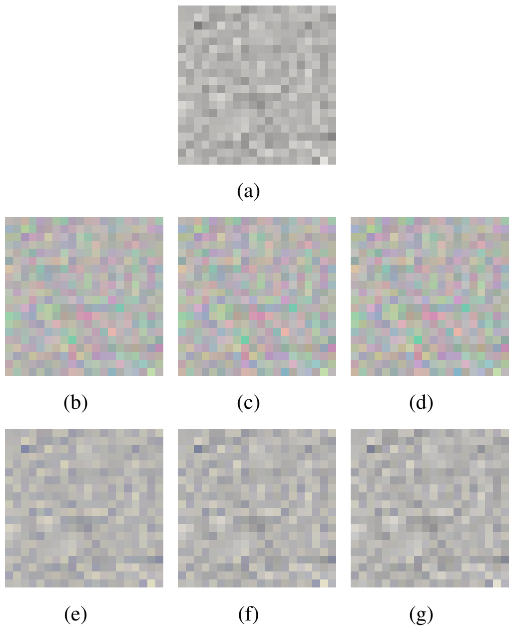

Fig. 3. Reference multispectral image constituted of random Gaussian noise (a) and images of this noise distorted using a bilinear interpolation (b), a bicubic interpolation (c) and a spline interpolation (d). The images of the noise re-corrected with the three same interpolation methods are shown respectively in (e), (f) and (g).

The advantage of this artificial multispectral image is that it has been generated considering only the transversal aberrations. The longitudinal aberrations explained in the introduction of this paper and causing shifts of the focal planes for the different color channels are not taken into account. In *real* multispectral images, they have a great impact on the blur that can not be separated from the blur coming from the interpolation step in the compensation of the transversal aberrations. This means that the blurring obtained with this artificial multispectral image comes only from the compensation of the transversal aberrations and not from the longitudinal aberrations.

We then distorted the reference multispectral image using some transformation matrices comparable to those obtained for real multispectral images. For the application of the transformation matrix and the interpolation required in order to calculate the gray values for each pixel position, we used the three interpolations explained in Sec. 2.3. The results of the distortion of the noise image are shown in Fig. 3(b) to 3(d). Those distorted multispectral images were then undistorted using the same interpolation methods as for the distortion step, see Fig. 3(e) to 3(g).

The compensated multispectral images are more blurred than the reference noise image on Fig. 3(a). The quality of the different interpolation methods are compared in Tab. 1 using the root mean square error (RMSE) and the mean value of the absolute differences (MAD) between the reference noise multispectral image and the multispectral images that have been distorted and then compensated. The gray values were coded with double precision between 0 and 1. As can be seen in the table, the bilinear interpolation leads to the worst values: the RMSE is 20% larger than the RMSE obtained with the spline interpolation and the MAD is 71% larger than with the spline interpolation when the bilinear interpolation is used. The results of bicubic interpolation are barely higher than with the spline interpolation.

Interpolation	RMSE	MAD
Bilinear	0.0530	0.0248
Bicubic	0.0466	0.0172
Spline	0.0441	0.0145

Tab. 1. Root mean square error (RMSE) and mean value of the absolute difference (MAD) between the noise pattern from Fig. 3(a) and the images distorted and then re-corrected using the three interpolation methods: bilinear, bicubic and spline.

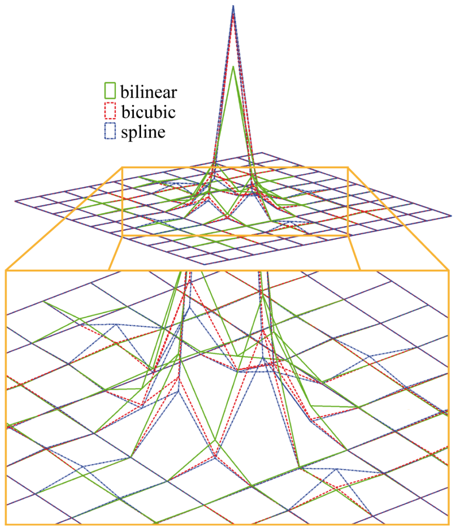

Fig. 5. PSFs of an image block distorted and corrected using the bilinear interpolation (in green), the bicubic interpolation (in red) and the spline interpolation (in blue).

The results of the three interpolations were also compared using the entropy of the multispectral images. Since we used an image of Gaussian noise, the entropy should be large. We therefore calculated the difference of the entropy of a channel in the reference noise image and of the entropy of the corresponding color channel in an image distorted and compensated as explained before. The results shown in the table in Fig. 4 lead to the same conclusion than with the RMSE and the MAD. The entropy obtained with the bilinear interpolation in the compensation step is much smaller than the one obtained with either the bicubic or the spline interpolation for each of the six channels. Moreover, the entropy of the images compensated with the spline interpolation is nearly always the closest to the entropy of the reference noise image. The only exception is the color channel with central wavelength 650 nm, for which the bicubic interpolation gives the closest result.

We also considered the distortion of the image and the compensation of this distortion as a system and analyzed the point spread function (PSF) of this system to evaluate the blurring it causes on the multispectral image. The PSF of a noise image can be calculated by transforming the image obtained at the output of the system and the original noise image into the frequency domain and by dividing them. These operations are performed on small blocks of the image, because the PSF of an optical system is a function of the position in the image. More details about the direct calculation of the PSF with a noise image can be found in [11]. The PSFs of the three systems using the bilinear, the bicubic and the spline interpolation are shown in Fig. 5 for a given image block and a given color channel. The low pass character of the three interpolation methods is made obvious by the wide shape of the PSFs. The impact of the PSF of the bilinear interpolation is even wider than the other ones, images compensated with the bilinear interpolation will thus be less sharp.

4. Effects of Interpolation on Color Accuracy

Besides the blur in compensated images, we also evaluated the relation between color accuracy and interpolation utilized for the compensation of the transversal aberrations. To this end, we acquired a multispectral image of a ColorChecker SG color chart, see Fig. 6. This section thus deals with a *real* multispectral image, in which transversal *and* longitudinal aberrations are present, and whose aim is to reproduce the acquired spectral stimuli faithfully. We compared the color patches in the three undistorted images with their spectra measured using a spectrophotometer.

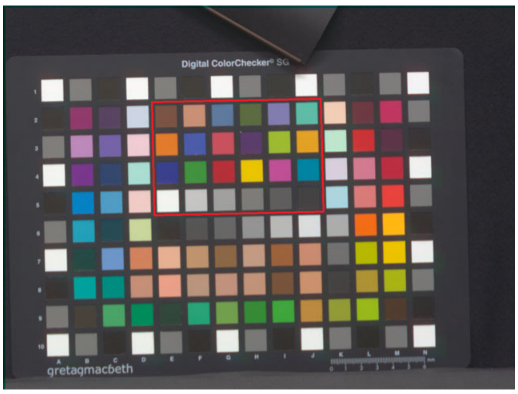

Fig. 6. ColorChecker SG target and the 24 color patches that were used to evaluate the quality of the three interpolation methods (inside the red frame).

Let us note m_s the acquired multispectral image, which contains aberrations that have to be compensated, and m_{lin} (resp. m_{cub} and m_{spl}) the multispectral image compensated using a bilinear interpolation (resp. a bicubic and a spline interpolation). $m_s(x, y, \lambda)$ then represents the pixel from the acquired multispectral image which is located at the position (x, y) in the color channel with the central wavelength λ.

Interpolation	Difference of entropy for the color channel with central wavelength					
	400 nm	450 nm	500 nm	600 nm	650 nm	700 nm
Bilinear	0.8512	0.9231	0.8427	0.3964	0.0730	0.9233
Bicubic	0.4029	0.4325	0.3935	0.1466	-0.0253	0.4376
Spline	0.2427	0.2741	0.2472	0.0875	-0.0320	0.2629

Fig.4. Difference of the entropy of the reference noise image and of the images distorted and compensated using the three interpolation methods, calculated separately for each color channel. A negative value means that the entropy of the compensated color channel is smaller than the entropy of the corresponding channel in the reference multispectral image. The values for the reference channel (550 nm) are not written since no transformation is performed for this color channel.

The pixels from the color patch number j from this image can be written

$$p_s^j = \{m_s(x,y,\lambda)\,|(x,y) \in \text{patch } j\} \ . \qquad (5)$$

Similar definitions apply to p_{lin}^j, p_{cub}^j and p_{spl}^j. $p_s^j(x,y)$ is then a vector of size $1 \times 1 \times 7$ representing the spectral values of the pixel (x,y) belonging to the color patch j.

For the evaluation of differences between two spectral stimuli, several formulae have been developed by the Commission Internationale de l'Eclairage over the years. The one we utilize in this paper is CIEDE2000, noted ΔE here. This color difference formula was published in 2001 and accounts for the color perception of a standard observer [12]. When the color difference ΔE between two color patches is below 1, no difference can be seen between them.

We considered separately each of the 24 color patches marked in the red frame in Fig. 6. We calculated the value $\Delta E(p_{\text{lin}}^j(x,y))$ of the color difference at the position (x,y) in the patch j in the multispectral image compensated using the bilinear interpolation, with regard to the measured spectra of the color patch. We repeated this for the bicubic and for the spline interpolation. For each pixel (x,y) belonging to the color patch j, we then compared $\Delta E(p_{\text{lin}}^j(x,y))$, $\Delta E(p_{\text{cub}}^j(x,y))$ and $\Delta E(p_{\text{spl}}^j(x,y))$ to know the best interpolation (the one leading to the lowest value of ΔE) and the worst interpolation (the one leading to the highest value of ΔE). The number of pixels for which each interpolation lead to the best and to the worst results are shown in Fig. 7. With the bicubic and the spline interpolation (blue and red lines), the number of pixels with the worst color accuracy (dotted lines) is often or even always larger than the number of pixels with the best color accuracy (solid lines). This means that these interpolation methods give more often the worst results than the best results. On the contrary, with the bilinear interpolation, the number of pixels with the best color accuracy is almost always larger than the number of pixels with the worst color accuracy. The bilinear interpolation thus seem to be more stable and should be chosen to achieve the most spectrally accurate multispectral acquisition.

In order to take the perceptual difference over the *whole* color patch into account, we also calculated the values $\Delta E(p_{\text{lin}}^j)$, $\Delta E(p_{\text{cub}}^j)$ and $\Delta E(p_{\text{spl}}^j)$, which are respectively the mean values of $\Delta E(p_{\text{lin}}^j(x,y))$, $\Delta E(p_{\text{cub}}^j(x,y))$

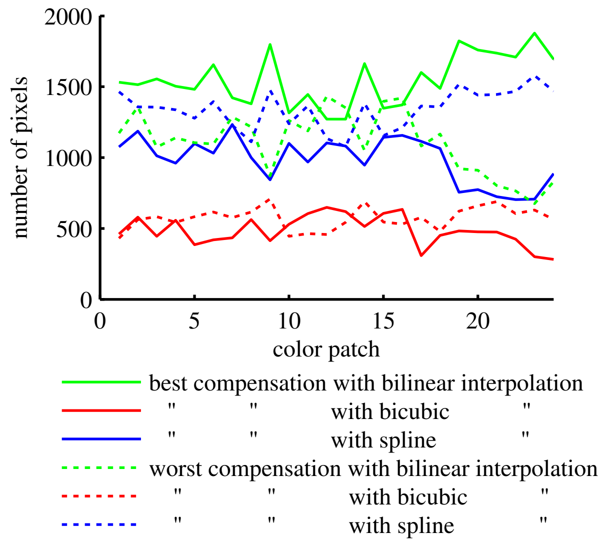

Fig. 7. Analysis of the perceptual differences ΔE of 24 fields from the ColorChecker SG. For each patch separately, we compared pixel wise which of the three interpolation methods leads to the best reconstruction and counted those pixels; this number of pixel is displayed here using solid lines. The dotted lines represent the number of pixels for which the interpolation leads to the worst reconstruction.

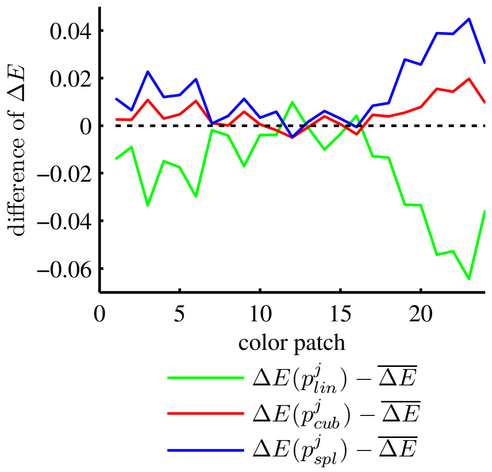

Fig. 8. Comparison of the perceptual differences ΔE of the color patches from the images compensated using the three different interpolation methods. The mean value $\overline{\Delta E}$ over the interpolations is subtracted from the perceptual differences for a better visualization of the results.

and $\Delta E(p^j_{\mathrm{spl}}(x, y))$ over the patch j. We then subtracted the mean value

$$\overline{\Delta E} = \frac{1}{3} \cdot \left(\Delta E(p^j_{\mathrm{lin}}) + \Delta E(p^j_{\mathrm{cub}}) + \Delta E(p^j_{\mathrm{spl}}) \right) \quad (6)$$

as shown in Fig. 8. The bilinear interpolation led to the best color accuracy for 22 over 24 color patches. Although, the range of the differences of ΔE lies between -0.064 and $+0.045$: these values are low and do not really correspond to perceptible differences. The results concerning the color accuracy should thus be considered with care and confirmed by other measurements.

5. Conclusions

We briefly explained how transversal aberrations in multispectral imaging can be measured and compensated and which role the interpolation step plays during the compensation. We then analyzed the effects of three interpolation methods – the bilinear, the bicubic and the spline – on the multispectral images obtained after compensation. The interpolation, through its low pass characteristic, cause a blurring of the compensated images. We measured the blur on a noise image and evaluated it using the root mean square error, the mean of absolute differences and the entropy. We also calculated the point spread function of the compensation system and found out that the spline interpolation leads to the sharpest noise image, the bilinear interpolation leading to the most blurred one. The blur of the different color channels in multispectral images is also harmful to their color accuracy. We compared the color difference between the compensated images and spectral measurements: the multispectral image compensated with the bilinear interpolation was perceptually closer to the real colors of the acquired target.

Acknowledgements

The author would like to thank Prof. Dr.-Ing. Til Aach, Institute of Imaging and Computer Vision, RWTH Aachen University, Germany, for supervising this project and the German Research Foundation for funding (DFG, grant AA5/2–1).

References

[1] BURNS, P.D., BERNS, S. Analysis Multispectral Image Capture. In *IS&T/SID 4th Color Imaging Conference*. Scottsdale (USA), November 1996, p. 19–22.

[2] HELLING, S., SEIDEL, E., BIEHLIG, W. Algorithms for Spectral Color Stimulus Reconstruction with a Seven-Channel Multispectral Camera. In *IS&Ts 2nd European Conference on Color in Graphics, Imaging, and Vision*. Aachen (Germany), April 2004, p. 254–258.

[3] MANSOURI, A., MARZANI, F.S., HARDEBERG, J.Y., GOUTON, P. Optical Calibration of a Multispectral Imaging System based on Interference Filters. *SPIE Optical Engineering*, 2005, vol. 44, no. 2, p. 027004.1–027004.12.

[4] LUTHER, R. Aus dem Gebiet der Farbreizmetrik. *Zeitschrift für technische Physik*, 1927, vol. 8, p. 540–558.

[5] KLEIN, J., BRAUERS, J., AACH, T. Methods for Spectral Characterization of Multispectral Cameras. In *IS&T/SPIE Electronic Imaging: Digital Photography VII*. San Francisco (USA), January 2011, p. to appear.

[6] BRAUERS, J., SCHULTE, N., AACH, T. Multispectral Filter-Wheel Cameras: Geometric Distortion Model and Compensation Algorithms. *IEEE Transactions on Image Processing*, 2008, vol. 17, no. 12, p. 2368–2380.

[7] BRAUERS, J., AACH, T. Longitudinal Aberrations Caused by Optical Filters and Their Compensation in Multispectral Imaging. In *IEEE International Conference on Image Processing*. San Diego (USA), October 2008, p. 525–528.

[8] TSAO, J. Interpolation Artifacts in Multimodality Image Registration Based on Maximization of Mutual Information. *IEEE Transactions on Medical Imaging*, 2003, vol. 22, no. 7, p. 854–864.

[9] ROHDE, G.K., ALDROUBI, A., HEALY JR., D.M. Interpolation Artifacts in Sub-Pixel Image Registration. *IEEE Transactions on Image Processing*, 2009, vol. 18, no. 2, p. 333–345.

[10] UNSER, M. Splines: a Perfect Fit for Signal and Image Processing. *IEEE Signal Processing Magazine*, 1999, vol. 16, no. 6, p. 22–38.

[11] BRAUERS, J., AACH, T. Direct PSF Estimation Using a Random Noise Target. In *IS&T/SPIE Electronic Imaging: Digital Photography VI*. San Jose (USA), January 2010, p. 75370B-1–75370B-10.

[12] CIE. *Improvement to Industrial Colour-Difference Evaluation*. CIE Publication no. 142-2001, Central Bureau of the CIE, Vienna, January 2001.

About Authors...

Julie KLEIN was born in 1984 in Haguenau, France. She received her engineering diploma from the Ecole Centrale Marseille, France, and her diploma degree in electrical engineering and information technology from the Technische Universität München, Germany, in 2008. She is currently working at the Institute of Imaging and Computer Vision, RWTH Aachen University, Germany, as a Ph.D. student. Her work focuses on image processing and multispectral imaging, in particular the analysis and the compensation of aberrations in multispectral cameras.